Supplement of Geosci. Model Dev., 19, 2985–3033, 2026
https://doi.org/10.5194/gmd-19-2985-2026-supplement

Geoscientific Model Development Open Access EGU

Supplement of

The coupled Southern Ocean–Sea ice–Ice shelf Model (SOSIM v1.0): configuration and evaluation

Chengyan Liu et al.

Correspondence to: Chengyan Liu (liuchengyan@sml-zhuhai.cn) and Zhaomin Wang (wangzhaomin@sml-zhuhai.cn)

Sect. S1 Topography construction workflow

The topography datasets for SOSIM were derived from the Refined Topography dataset version 2 (RTopo-2), which provides consistent topography of bedrock, elevation, and ice draft on a spherical grid. The workflow for constructing the model topography is as follows.

1) The RTopo-2 data south of 35°S (43201 × 6601 cells, 30 arcsec resolution) is interpolated onto the SOSIM orthogonal curvilinear grid (1800 × 1800 cells, ~5 km resolution) using a nearest neighbour scheme. This approach preserves the original values without smoothing but can introduce artifacts in regions with complex coastlines or steep topographic gradients.

2) After remapping, a thorough inspection of the resulting topography fields is performed to identify problematic isolated wet cells that were disconnected from the main ocean domain (e.g., enclosed by dry land or ice shelves with no flow pathway). Since the model applies additional constraints during initialization, such as minimum water column thickness requirements and partial-cell adjustments, the model modifies the actual distribution of wet cells relative to the raw input topography. Therefore, the identification of isolated cells should be based on the mask file generated by the model (e.g., the 'hFac' file) rather than on the theoretical water column thickness (ice draft minus bedrock depth). The mask file can be generated by running the model for one time step without additional components (e.g., sea ice, atmospheric forcing, and open boundary forcing).

3) Problematic cells are corrected through a manual editing process. The edits of the bedrock depth and ice draft mainly focus on removing isolated wet cells by converting them to dry cells. The manual edits are concentrated in regions with complex coastal geometry, particularly around the Antarctic Peninsula, the sub-Antarctic islands (e.g., South Shetland Islands and South Orkney Islands), and the margins of large ice shelves (e.g., the Ross Ice Shelf and Filchner-Ronne Ice Shelf). The revised topography is then used to generate an updated mask file by running the model for a single time step.

4) The updated mask file is visually inspected again to ensure that the manual edits have not introduced unrealistic features or new isolated wet cells. If problematic cells are identified again, further modifications to the bedrock depth or ice draft are necessary, and the process of model re-runs and re-inspection is repeated. This iterative loop continues until all problematic cells are resolved in the final generated mask file. In total, ~0.15% of grid cells are manually adjusted in SOSIM v1.0.

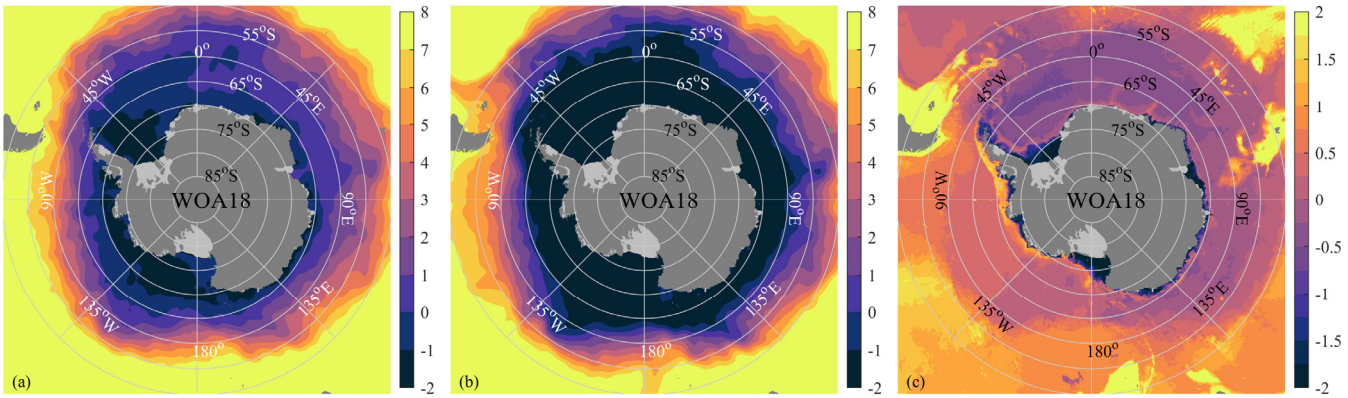

Fig. S1. The horizontal distribution of θ (°C). **(a)** Climatological SST in summer from WOA18. **(b)** As in **(a)**, but for SST in winter. **(c)** As in **(a)**, but for the climatological annual mean θ at the bottom layer.

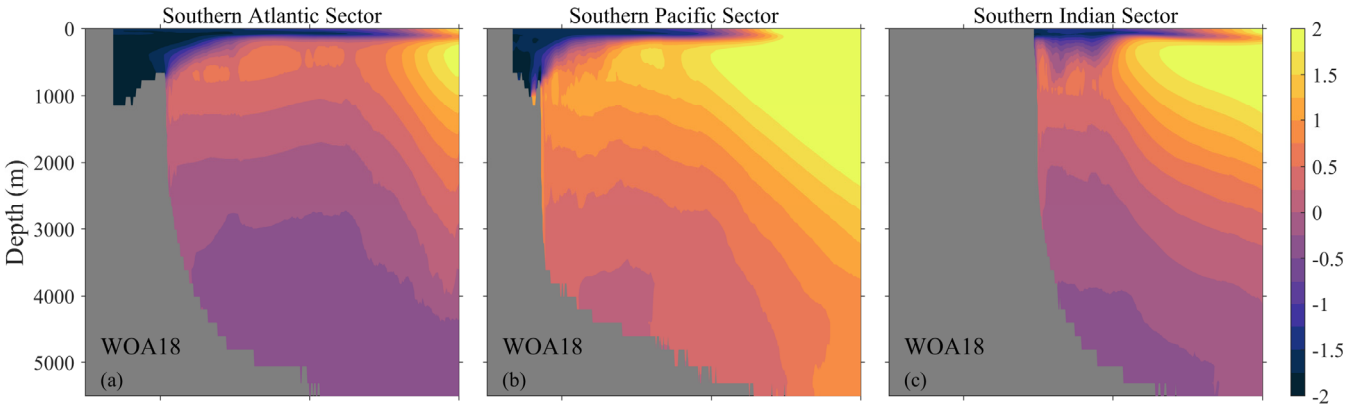

Fig. S2. The vertical distribution of zonally averaged θ (°C). **(a)** Climatological annual mean of zonally averaged θ in the Southern Atlantic sector from WOA18. The zonal average is calculated by omitting dry grids. **(b)** and **(c)** As in **(a)**, but for the Southern Pacific and Southern Indian sectors, respectively.

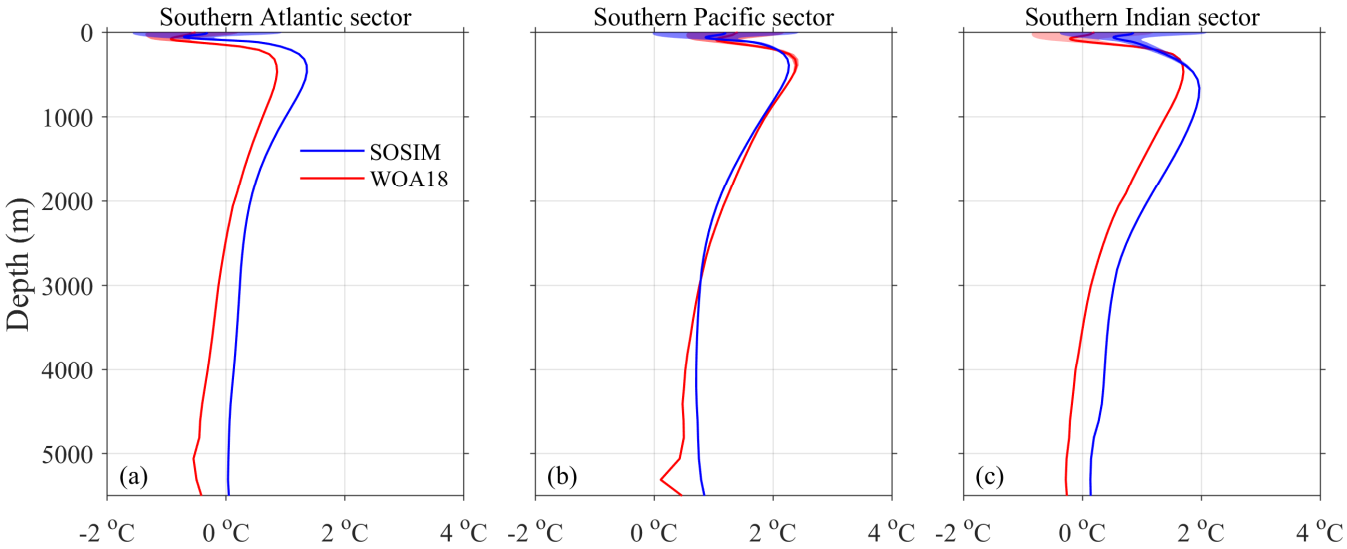

Fig. S3. The vertical profiles of horizontally area-averaged θ (°C). **(a)** The horizontally area-averaged θ within the Southern Atlantic sector (semi-transparent red region in Fig. 5a in the manuscript). Semi-transparent color shading denotes the STD of monthly climatology. **(b)** and **(c)** As in **(a)**, but for the Southern Pacific and Southern Indian sectors, respectively.

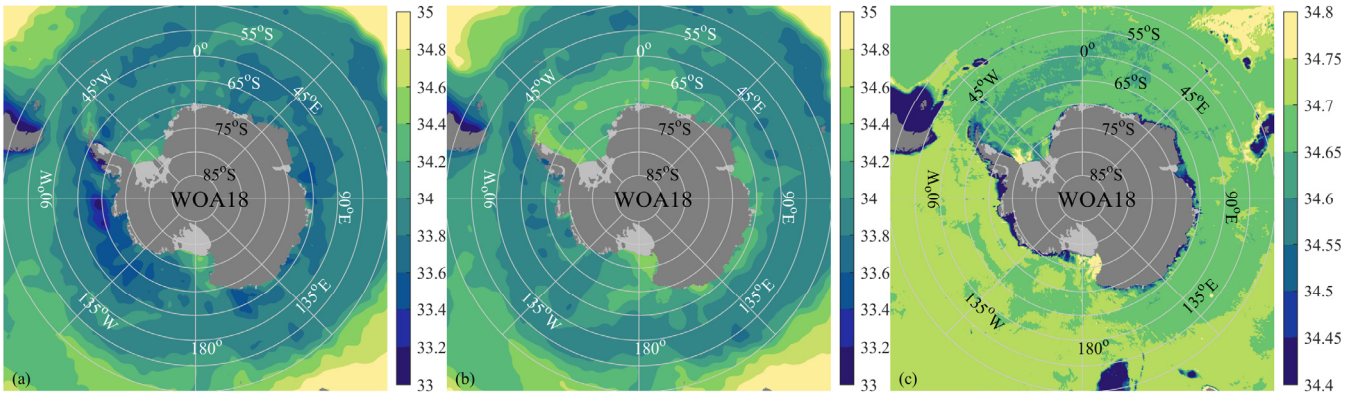

Fig. S4. As in Fig. S1, but for the horizontal distribution of *S* (psu).

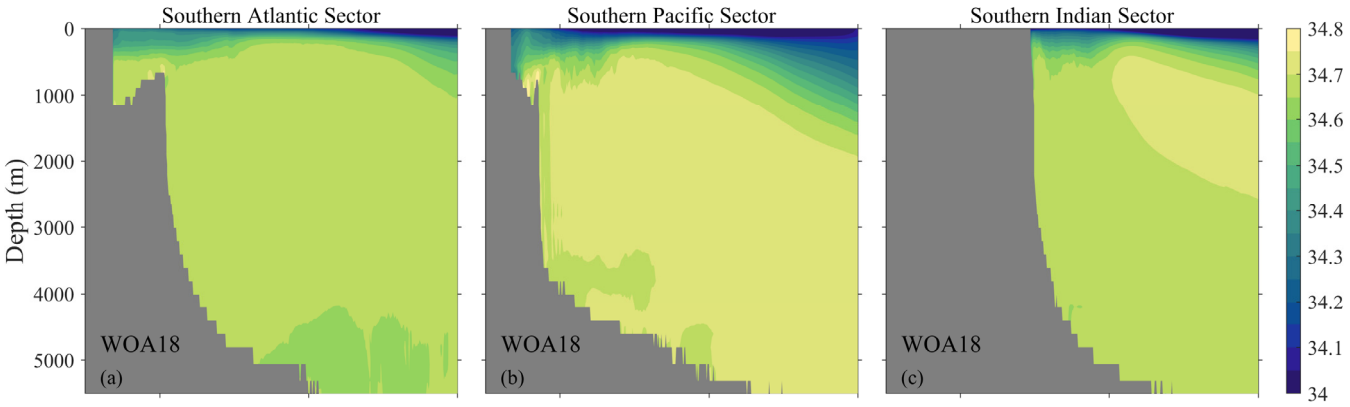

Fig. S5. As in Fig. S2, but for the vertical distribution of zonally averaged *S* (psu).

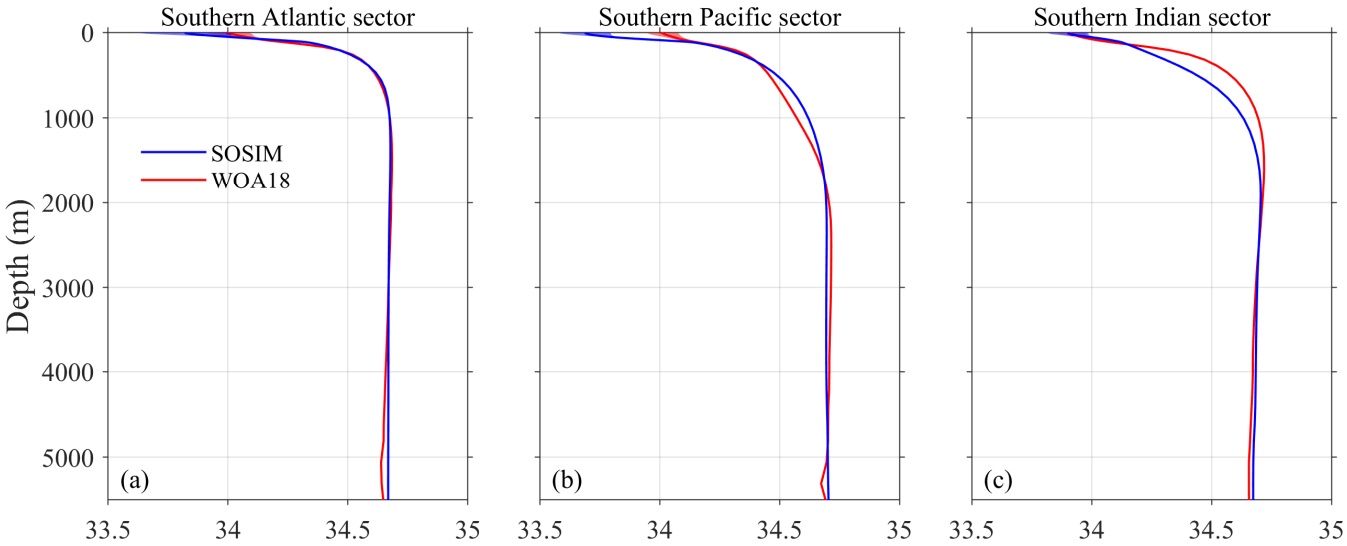

Fig. S6. As in Fig. S3, but for the horizontally area-averaged *S* (psu).

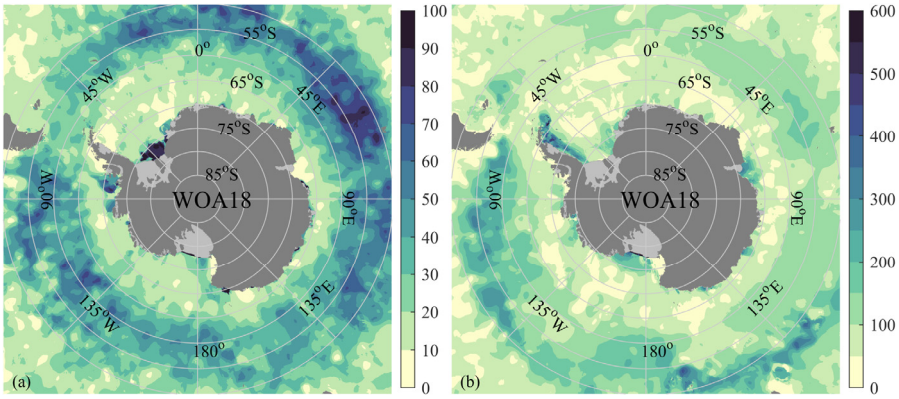

Fig. S7. The horizontal distribution of MLD (m). **(a)** The MLD of WOA18 in the austral summer. **(b)** As in **(a)**, but for the MLD in the austral winter.

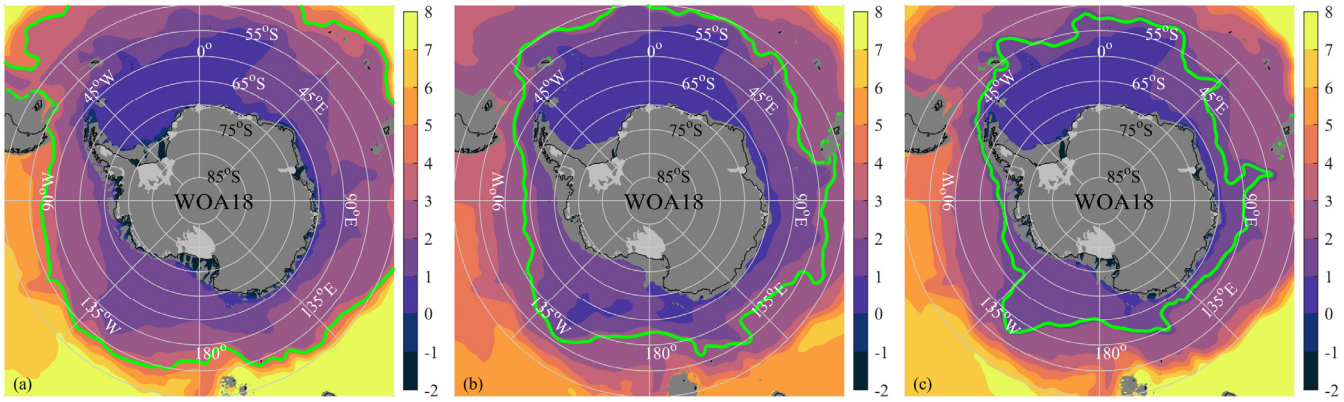

Fig. S8. The circumpolar distribution of the SAF, PF, and SACCF in WOA18, with θ (°C) at corresponding depths in color. **(a)** The SAF (the green line, 4 °C isotherm) and θ (°C) at 400 m depth. **(b)** As in **(a)**, but for the PF (2.2 °C isotherm) and θ (°C) at 800 m depth. **(c)** As in **(a)**, but for the SACCF (1.8 °C isotherm) and θ (°C) at 500 m depth.

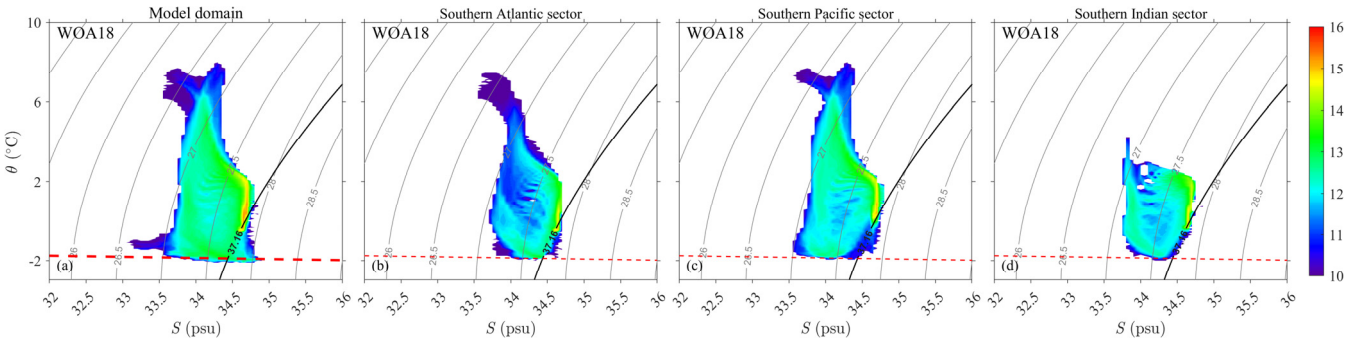

Fig. S9. (a) Climatological water mass volume (log10 (V), m^3) distribution in θ–S space (bins of 0.05 °C by 0.05 psu size) in the inner model domain in WOA18, superimposed with potential density σ_0 (grey lines) in contour intervals of 0.5 kg m^{-3}. The red dashed line denotes the surface freezing point of seawater. The black lines denote the σ_2 contours of 37.16 kg m^{-3}, indicating the threshold between CDW and AABW. **(b-d)** As in **(a)**, but for the Southern Atlantic sector, the Southern Pacific sector, and the Southern Indian sector, respectively.

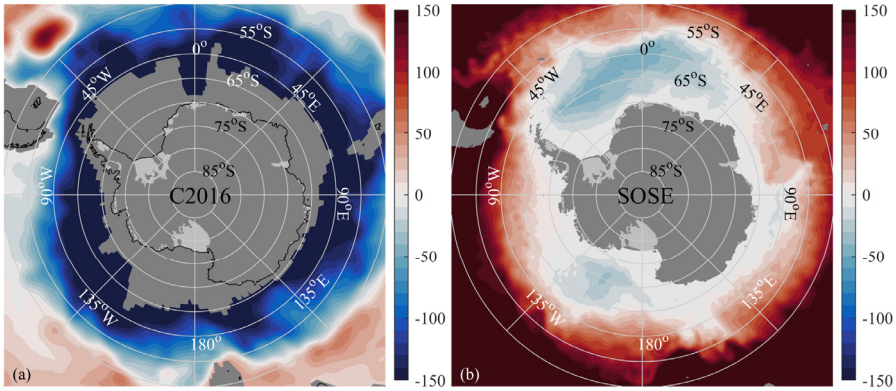

Fig. S10. The barotropic stream function. **(a)** The climatological Ψ (Sv) estimated from the C2016. The grey region over the open ocean indicates the absence of observational estimation. **(b)** As in **(a)**, but for SOSE. Negative cells denote cyclonic circulations.

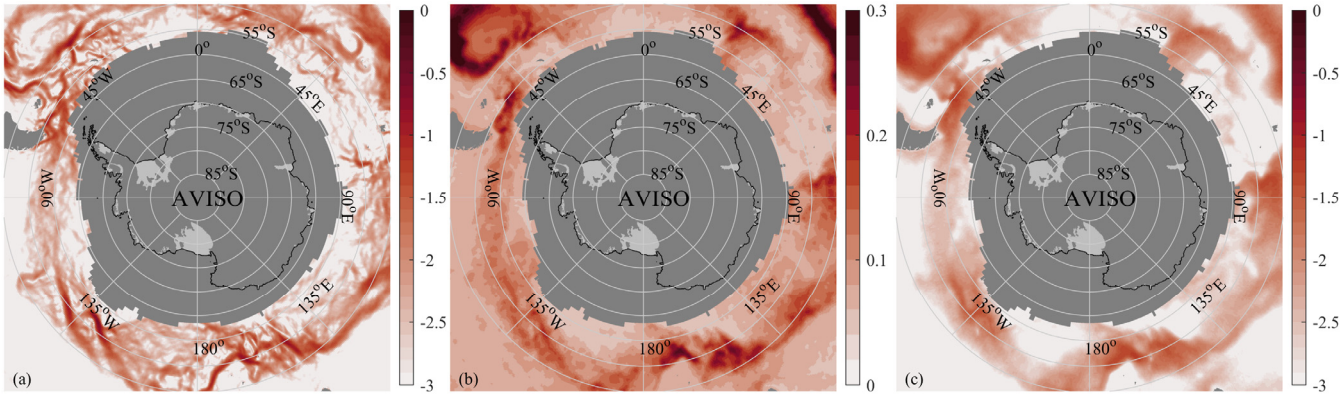

Fig. S11. The sea surface Kinetic Energy and the variability of η. **(a)** The $\log_{10}(MKE_{surf})$ (m^2 s^{-2}) in the AVISO. The grey region over the open ocean indicates the absence of year-round data in the AVISO. (b) and (a) As in (a), but for the STD of η (m) and the $\log_{10}(EKE_{surf})$ (m^2 s^{-2}), respectively.

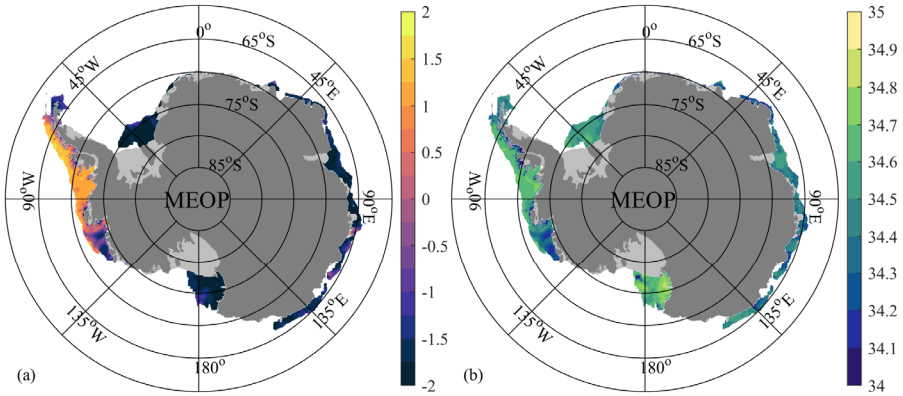

Fig. S12. The horizontal distribution of θ (°C) and S (psu) over the continental shelf. **(a)** Climatological θ at the bottom layer from the gridded MEOP. **(b)** As in **(a)**, but for bottom S.

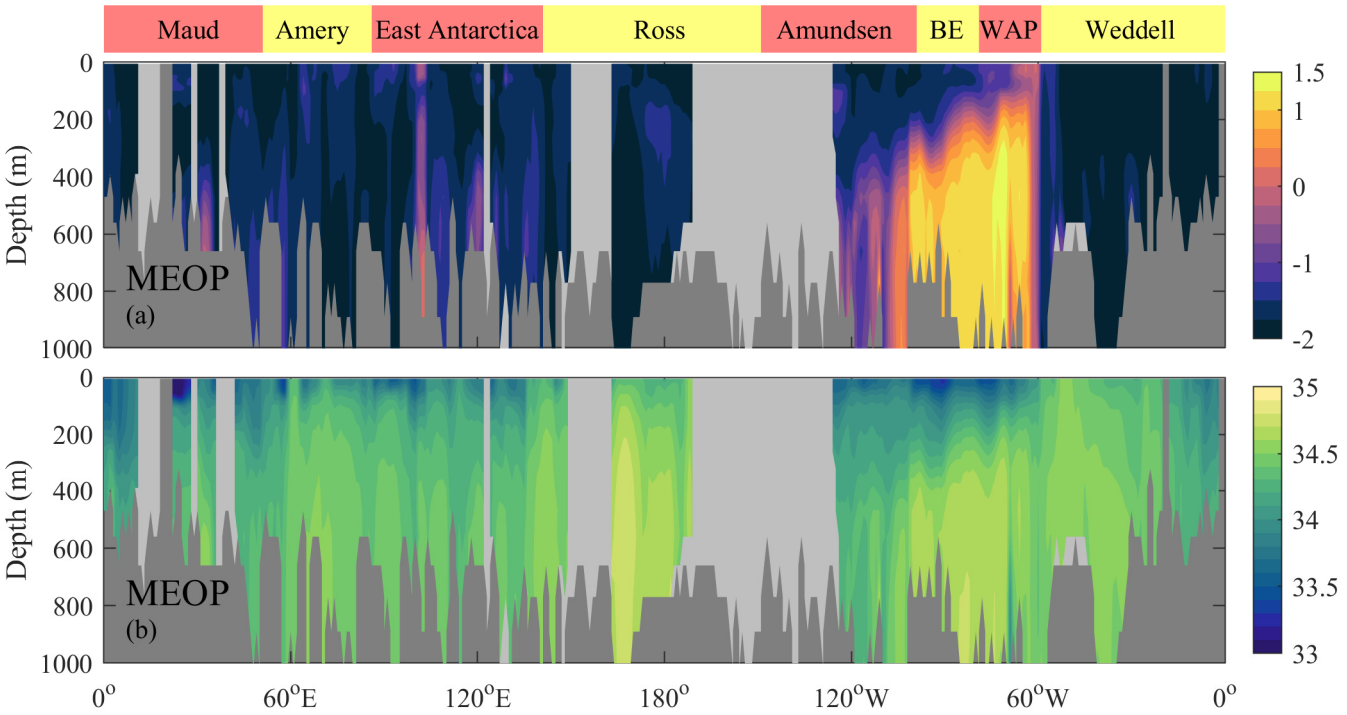

Fig. S13. The vertical structure of θ (°C) and S (psu) over the continental shelf. **(a)** Meridionally averaged θ over the continental shelf from the gridded MEOP. The light grey region indicates the absence of year-round data in the gridded MEOP. **(b)** As in **(a)**, but for S.

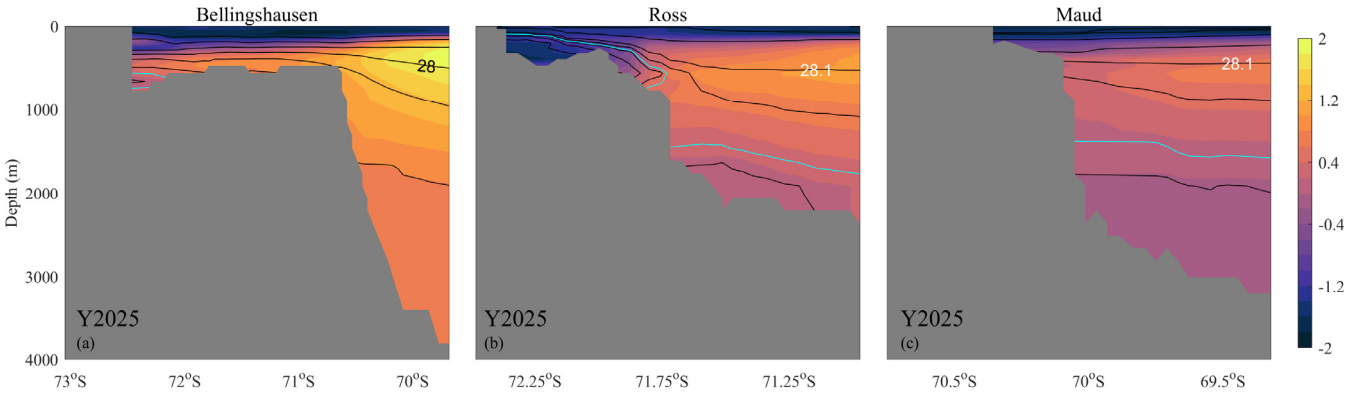

Fig. S14. The meridional structure of θ (°C) along the selected transects (blue lines in Fig. 5b) perpendicular to the continental slope. **(a)** Climatological θ along the selected transect in the Bellingshausen sector from Y2025. Black lines denote σ_0 (kg m^{-3}) in contour intervals of 0.1 kg m^{-3}. **(b)** and **(c)** As in **(a)**, but for the transects in the Ross and Maud sectors, respectively. The cyan lines denote the γ^n contour of 28.27 kg m^{-3}.

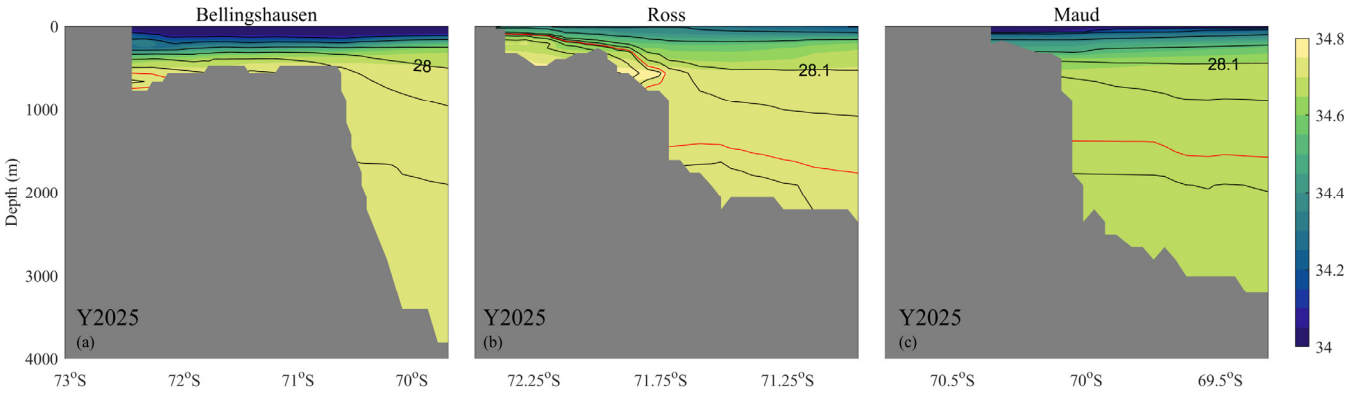

Fig. S15. As in Fig. S14, but for S (psu), with the red line denoting the γ^n contour of 28.27 kg m^{-3}.

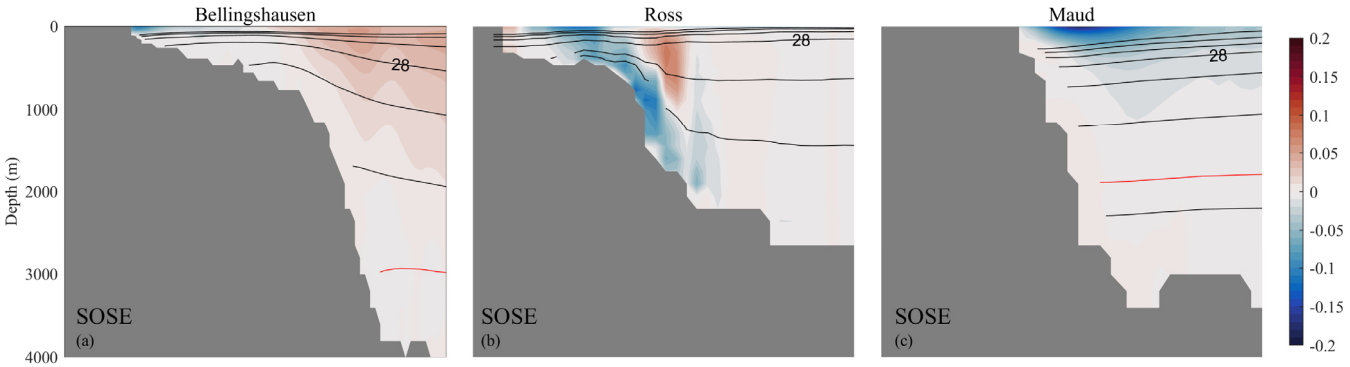

Fig. S16. The meridional structure of u_{along} (m s^{-1}) along the selected transects (blue lines in Fig. 5b) perpendicular to the continental slope. **(a)** Climatological u_{along} along the selected transect in the Bellingshausen sector from the SOSE. Positive values indicate a current flowing to the right of the down-slope direction (i.e., a generally eastward-flowing ASC). Black lines denote σ_0 (kg m^{-3}) in contour intervals of 0.1 kg m^{-3}. The red line denotes the γ^n contour of 28.27 kg m^{-3}. **(b)** and **(c)** As in **(a)**, but for the transects in the Ross and Maud sectors, respectively.

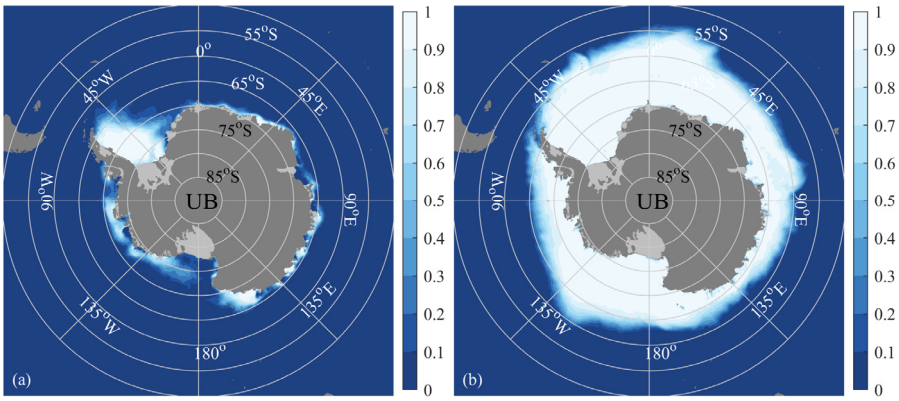

Fig. S17. The spatial pattern of SIC. **(a)** The satellite observed SIC in February from the UB. **(b)** As in **(a)**, but for September.

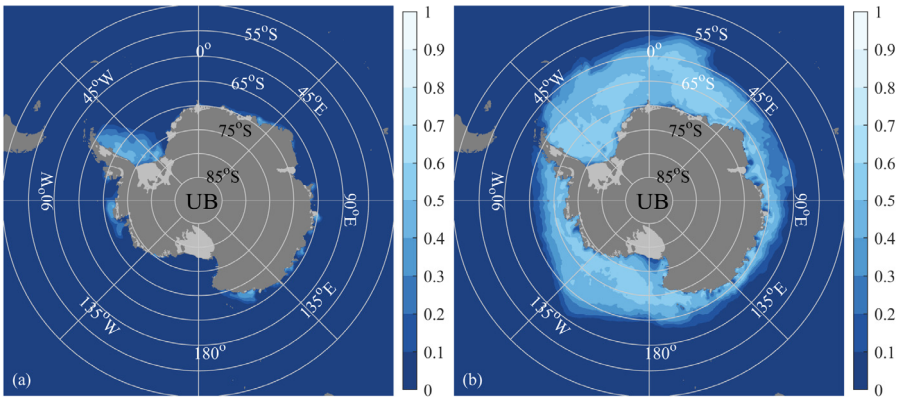

105 **Fig. S18.** As in Fig. S17, but for the SIT (m).

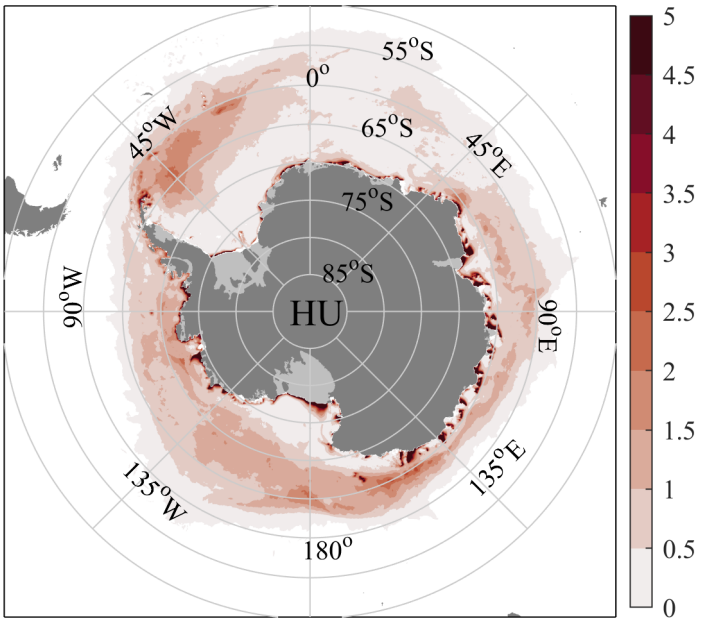

Fig. S19. The spatial pattern of estimated SIP (m yr^{-1}) during the freezing period (March-October) based on the AMSR-E by the HU.

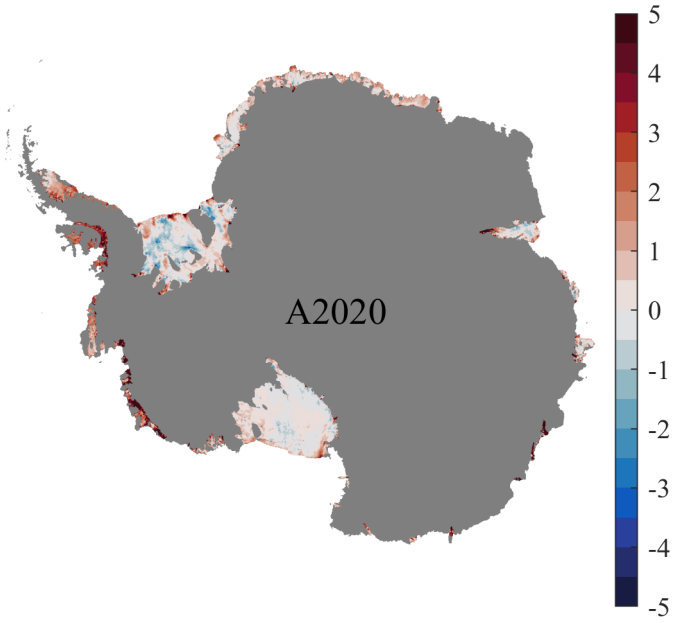

Fig. S20. The observed annual climatology of spatial pattern of SHI_{fw} (m yr^{-1}) from A2020.